JSR Publications

Available Online

J. Sci. Res. **17** (1), 9-19 (2025)

JOURNAL OF SCIENTIFIC RESEARCH

www.banglajol.info/index.php/JSR

Space Tether Dynamics and Stability of Equilibrium Positions under Different Perturbative Forces of General Nature in the Central Gravitational Field of Earth

J. Ghosh[1*], S. Kumar[2]

[1]P. G. Department of Physics, R. D. S. College, B. R. A. Bihar University, Muzaffarpur-842002, India

[2]P. G. Department of Physics, L. S. College, B. R. A. Bihar University, Muzaffarpur-842001, India

Received 1 March 2024, accepted in final revised form 12 October 2024

Abstract

This paper presents an analysis of the stability of equilibrium positions of two artificial satellites system connected by light, flexible and elastic long tether under the combined effect of several classical perturbative forces in elliptical orbit. The tether may be either conducting or non-conducting. In this study, it is assumed to be non-conducting in nature. We have treated the problem with taking five perturbative forces acting simultaneously on the system. Among these perturbations, three perturbations exist due to the Earth's influences: the geomagnetic field, shadows and oblateness. The other two perturbations are due to the elasticity of the cable and solar light pressure. The effect of air resistance is neglected considering the satellites as high-altitude satellites. To determine the stability of the satellites, the Lyapunov method has been used. The dynamical behaviours of the satellites are represented by differential equations. As anticipated, the Lyapunov method indicates that the equilibrium position is unstable. At last we have neglected the perturbative forces and treated the problem only under the effect of central gravitational field. The stability analysis is then carried graphically, and final conclusions are drawn.

Keywords: Tether; Satellites; Shadow; Oblateness; Geomagnetic field; Solar light pressure.

doi: https://dx.doi.org/10.3329/jsr.v17i1.71710 J. Sci. Res. **17** (1), 9-19 (2025)

1. Introduction

Space tethers are long cables which connect the end bodies, satellites, space stations to each other in space. The cable may range from a few hundred meters to several kilometers in length and typically possesses properties such as high tensile strength, low-density and a small diameter. The cable may be either conductive or non-conductive. When the core of the cable is conductive, it is called electrodynamic tether. The conductive tether interacts with the geomagnetic field and can generate electricity by electromagnetic induction. If the

* *Corresponding author*: joydip.ghosh1990@gmail.com

core of the cable is non-conductive, it is called non-electrodynamic tether and also has many potential applications in space technology. The other category of tethers is momentum exchange tethers. It may be rotating or non-rotating. When multiple space vehicles are connected by non-conductive tethers it is technically termed as tether formation flying. The main difference of tether satellites with the conventional space satellites are of its long length, variable in configuration and geomagnetic interaction. It is also to be noted that depending upon the configuration of tether it can be divided into two systems namely static system and dynamic system. In a static system, the length of the tether, the relative position of the objects and their orientation do not change over time. In dynamic systems, the configuration and structure of the system change significantly.

Although the idea of space tether is more than a century old, with credit going to Tsiolkovsky [1], many of its applications are still in the theoretical domain, with only a few tested experimentally. The main technical difficulties are still in tether materials for very long cables and its controls. The satellites system is exposed by several perturbative forces during the motion other than earth's gravitational field. The conservative perturbative forces are earth's oblateness, lunar attraction, solar attraction, planetary attraction, tidal effect, relativistic effects and so on. The non-conservative perturbative forces are atmospheric friction, solar radiation pressure, albedo effect, earth's magnetic field and so on. The elasticity of the cable also acts as a perturbation on the system. These several perturbative forces act as a damping force on the system and make the system unstable. In this paper, we will discuss about the stability of the system by taking five perturbative forces simultaneously on the system and finally without the perturbative forces.

With the help of the tether satellites system, a wide range of problems can be solved that are not possible by conventional satellites. Some of the most interesting applications are given here. It can be used to create artificial gravity on board a space station and exactly for this reason the use of tether satellite system was first proposed. This was tested in Gemini -11 mission in 1966 by NASA. In this mission the spacecraft was connected via a 30 m space tether. By rotating this system around the common centre of mass with an angular velocity of $1.6 \times 10^{-4}\ s^{-1}$, an artificial gravity of 10^{-4} g was generated. Such a low value of gravity may be useful for transmission of fuel from one spacecraft to another [2]. The other applications are lifting of spacecraft to higher orbit with a rotating space tether, use as a space escalator, space elevator, studying the upper atmosphere, generation of electrical energy by conductive tether, space debris collection and many more. In astronautics, it is a common practice of space flight between various orbits. To do this the jet engine is used for providing impulse to the system. By using a rotating space tether, a payload can be transferred to higher orbit without any fuel or jet engine. A large amount of theoretical work has been devoted to the study of the space elevator [3,4], although it requires immense effort and poses manufacturing challenges. By connecting a tethered probe from a base spacecraft is a solution to study the atmosphere at an altitude 100-200 km as conventional satellites cannot work effectively at this height [5]. By moving a conductive tether in geomagnetic field, a voltage can be developed according to the laws of electromagnetic induction. Its value is proportional to the conductor length, magnetic field

induction and speed of the conductor. In 1996, the TSS-1R experiment was carried out. A voltage of 3500 V was generated using a 19.7 km electrodynamic tether. However, an electrical arc caused a break in the tether due to an isolation fault. The generated power exceeded the expected value many times over [6].

The study of the stability of satellite system is very important to make operate space tether normally in orbit. Unstable systems can lead to failure due to the tether breaks or wind with the main satellites. For many applications, stationary movement of the tether is most suitable. In many studies of tether satellites, researchers have assumed that the satellite system moves in a circular orbit and have obtained valuable insights. The detailed investigation for searching stationary motion of tether and their stability was investigated by Beletsky and Levin [5]. They showed that in a circular orbit, the motion of the systems and its elastic vibrations are unstable. Kurpa *et al*. [7] studied the modelling, dynamics and control of tethered satellite systems. Khan and Goel [8] worked on the chaotic motion related to the dumbbell satellite problem. Kumar and Prasad [9] studied about the nonlinear planer oscillation of cable-connected satellite system and non-resonance. Kumar *et al*. [10] worked on the equilibrium positions of a cable-connected satellite systems under several influences. Kumar [11] worked on the liberation points of a cable-connected satellites system under the effect of solar radiation pressure, the earth's magnetic field, the shadow of the earth and air resistance in a circular orbit.

In most of the studies, stability problems are carried out in the absence of other generalized perturbing forces. The relative equilibriums and stability conditions for the tether satellites system were studied by Burov and Troger [12]. The method for solving the absolute stability of dynamical systems was studied by Liberzon [13]. Yu *et al*. [14] reviewed the dynamics, modelling and stability of tethered satellite systems. Yu *et al*. [15] also studied the chaotic motion of tethered satellite systems under the effect of air drag and earth's oblateness. The numerical investigation of the tether deployment process was analyzed by Mckenzie [16]. Malashin *et al*. [17] analyzed the stability of tether deployment for a particular trajectory based on the Lyapunov function. Jung *et al*. [18] studied the dynamics of a three-body tether satellite system. Pelaez and Andres [19] studied the stability problem for electrodynamic tethers in elliptical orbit. They showed that the motion is unstable due to the energy inflow caused by the geomagnetic field.

2. Mathematical Models of Space Tether

In the literature, significant attention has been given to the space tether dynamical model. The existing models can be categorized into three groups based on the nature of the tether. The models are heavy flexible thread model, discrete model and the massless thin tether model. Generally, the dynamical equations for these three models are constructed using Lagrange's equations [20], Hamilton's principle [21] and Newton's laws [22]. The degrees of freedom of the system are generally fixed in the popular models available for cable-connected satellites systems. Constraints are imposed on the system to reduce the degrees of freedom. A time varying number of degrees of freedom dynamical model was

constructed by Yu *et al*. [23]. These multiple degrees of freedom make the system very much complicated. The equations obtained under different perturbative forces of the tether satellites are generally nonlinear and non-autonomous. In this study, the rod model of tethered satellites system has been taken for analytical analysis.

The large number of models available is not only due to the various nature of the tether but also due to the presence of various perturbative forces. It is important to note that not all perturbative forces need to be considered in a single space tether model. Out of the several perturbations, the effect of earth's oblateness is the most significant one. The effect of atmospheric friction in low earth orbit is 10^{-3} times the effect of earth's gravity and totally negligible above 500 km of altitude. Although the effects of solar pressure and earth's magnetic field are small, they are considered because the system is exposed to these forces for extended periords during station-keeping phase. For rigid tether models, the effect of elasticity is negligible.

The satellite system is modeled as two mass points connected by a long elastic tether, which is light and non-conducting in nature. The system is treated as a high-altitude satellite system, and the effect of atmospheric drag is not taken into account. The system is analyzed under the combined influences of the shadow of the earth, solar radiation pressure, oblateness of the earth and earth's magnetic field. The shadow of the earth is taken as cylindrical in nature.

3. Equations of Motion

The differential equations of motion for the satellites system under the above-mentioned perturbative forces in rotating co-ordinate system (Fig. 1) in Keplerian elliptical orbit are written as [24]

$$\ddot{\xi} - 2\dot{\nu}\dot{\eta} - \ddot{\nu}\eta - \dot{\nu}^2\xi - \frac{2\mu}{R^3}\xi + \lambda_\alpha\left[1 - l_0\left(\xi^2 + \eta^2 + \tau^2\right)^{-1/2}\right]\xi =$$

$$-\left(\frac{m_1}{m_1+m_2}\right)\left(\frac{Q_1}{m_1} - \frac{Q_2}{m_2}\right)\left(\frac{\mu_E}{R^3}\right)(\cos i)R\dot{\nu} + \gamma\left(\frac{B_2}{m_2} - \frac{B_1}{m_1}\right)\cos\in\cos(\nu-\alpha) + \frac{12\mu k_2}{R^5}\xi$$

$$\ddot{\eta} + 2\dot{\nu}\dot{\xi} + \ddot{\nu}\xi - \dot{\nu}^2\eta + \frac{\mu}{R^3}\eta + \lambda_\alpha\left[1 - l_0\left(\xi^2 + \eta^2 + \tau^2\right)^{-1/2}\right]\eta$$

$$= -\left(\frac{m_1}{m_1+m_2}\right)\left(\frac{Q_1}{m_1} - \frac{Q_2}{m_2}\right)\left(\frac{\mu_E}{R^3}\right)\dot{R}\cos i + \gamma\left(\frac{B_2}{m_2} - \frac{B_1}{m_1}\right)\cos\in\sin(\nu-\alpha) - \frac{3\mu k_2}{R^5}\eta \tag{1}$$

The equations look like very much complicated. To simplify them, Nechvile's co-ordinate system is introduced. In this co-ordinate system, dilation is applied to the rotating co-ordinate system. The dilation is expressed as

$$\xi = \rho X, \quad \eta = \rho Y \tag{2}$$

Where X, Y are the co-ordinates in Nechvile's system.
Here,

$$\rho = \frac{R}{p} = \frac{1}{1 + e\cos\nu} \tag{3}$$

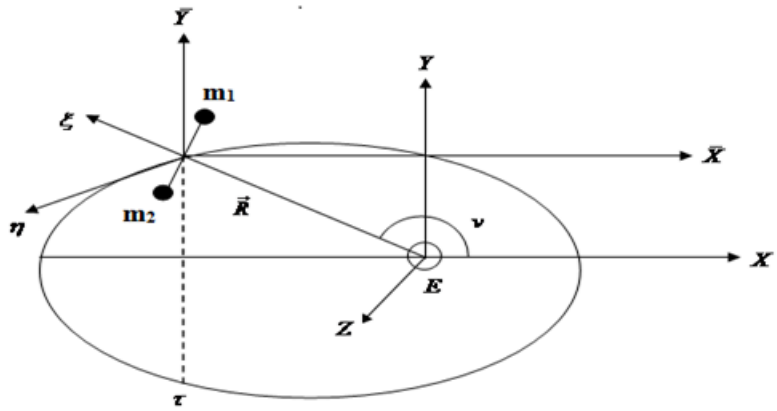

Fig. 1. Rotating co-ordinate configuration of space tether.

Putting equations (2) in equations (1) and doing some simplification, the equations (1) becomes

$$X''-2Y'-3X\rho=-\frac{A}{\rho}\cos i-\gamma\frac{R^3}{\mu}\left(\frac{B_1}{m_1}-\frac{B_2}{m_2}\right)\cos\in\cos(\nu-\alpha)+\frac{12k_2}{R^2}\rho X$$

$$-\lambda_\alpha\frac{R^3}{\mu}\left[\rho-l_0\left(X^2+Y^2\right)^{-1/2}\right]X$$

$$Y''+2X'=-\frac{A\rho'}{\rho^2}\cos i+\gamma\frac{R^3}{\mu}\left(\frac{B_1}{m_1}-\frac{B_2}{m_2}\right)\cos\in\sin(\nu-\alpha)-\frac{3k_2}{R^2}\rho Y$$

$$-\lambda_\alpha\frac{R^3}{\mu}\left[\rho-l_0\left(X^2+Y^2\right)^{-1/2}\right]Y \qquad (4)$$

Where, $\lambda_\alpha=\left[\frac{m_1+m_2}{m_1m_2}\right]\frac{\lambda}{l_0}$ $\qquad A=\left(\frac{m_1}{m_1+m_2}\right)\left(\frac{Q_1}{m_1}-\frac{Q_2}{m_2}\right)\frac{\mu_E}{\sqrt{\mu p}}$

Also, $k_2=\frac{\varepsilon R_e^{\ 2}}{3},\ \varepsilon=\alpha_R-\frac{m}{2},\ m=\frac{\Omega^2 R_e}{g_e}$

The following nomenclature for the above equations has been used:

Nomenclature: m_1 and m_2 are the masses of the two satellites, R is the magnitude of the radius vector $\bar{R}$. μ is a gravitation parameter and is the product of universal gravitational constant and earth's mass, λ is the elastic parameter of the cable. Q_1 and Q_2 are charges on m_1 and m_2 respectively, γ is a shadow function, it is zero when the satellites are affected by the earth's shadow otherwise its value is one. B_1 and B_2 are the absolute values of the forces due to the direct solar pressure, l_0 denote the original length of the cable, μ_E is the value of magnetic moment of the earth's dipole. ξ is the rotating co-ordinate and is along the direction of radius vector $\bar{R}$ and η is towards the transversal direction. ν is the true anomaly of the centre of mass of the system, i is the inclination of the orbit with the equatorial plane. ϵ is the inclination of the oscillatory plane of the masses m_1 and m_2 with the orbital plane of the centre of mass of the system. α is the inclination of the ray, e is the eccentricity of the

elliptical orbit, α_R is the earth's oblateness, Ω is the angular velocity of the earth's rotation, R_e is the equatorial radius of the earth and g_e is the acceleration due to gravity. The dot represents differentiation with respect to time and the prime represents the differentiation with respect to the true anomaly.

4. Equilibrium Positions of the System

During the motion, the entire system travels through earth's cylindrical shadow beam. Let, θ be the angle subtended by the axis of the shadow beam and the line connecting the centre of the earth and the end point of the orbit of the centre of mass. The system is under the impact of solar light pressure when it forms an angle θ with the axis of the shadow beam and remains under the impact of solar pressure until it forms an angle of (2π- θ) with the axis of the cylindrical shadow beam. The satellites will now enter within the shadow beam and the yield of radiation stops. In equations (4), the average of periodic terms is calculated with respect to υ from θ to (2π- θ), where the system is under the yield of the sun rays directly i.e. $\gamma = 1$ and from - θ to + θ, where the system moves through the shadow beam i.e. $\gamma = 0$. Averaging the effect of earth's shadow, the equations (4) becomes

$$X''-2Y'-\frac{3X}{\left(1-e^2\right)^{1/2}}=-A\cos i+\frac{R^3}{\mu}\left(\frac{B_1}{m_1}-\frac{B_2}{m_2}\right)\frac{\cos\in\cos\alpha\sin\theta}{\pi}+\frac{12k_2}{R^2}\frac{1}{\left(1-e^2\right)^{1/2}}X-$$
$$\lambda_\alpha\frac{1}{\left(1-e^2\right)^{1/2}}\frac{R^3}{\mu}\left[1-l_0\left(X^2+Y^2\right)^{-1/2}\right]X$$

$$Y''+2X'=\frac{R^3}{\mu}\left(\frac{B_1}{m_1}-\frac{B_2}{m_2}\right)\frac{\cos\in\sin\alpha\sin\theta}{\pi}-\frac{3k_2}{R^2}\frac{1}{\left(1-e^2\right)^{1/2}}Y-\lambda_\alpha\frac{R^3}{\mu}\frac{1}{\left(1-e^2\right)^{1/2}}\left[1-l_0\left(X^2+Y^2\right)^{-1/2}\right]Y \tag{5}$$

The solution of equations (5) is difficult. By considering the maximum effect of earth's shadow, these equations can be simplified. For this purpose, specific values $\in=0$ and $\alpha=0$ are applied in equations(5).

Hence, the equations (5) becomes

$$X''-2Y'-\frac{3X}{\left(1-e^2\right)^{1/2}}=-A\cos i+\frac{R^3}{\mu}\left(\frac{B_1}{m_1}-\frac{B_2}{m_2}\right)\frac{\sin\theta}{\pi}+\frac{12k_2}{R^2}\frac{1}{\left(1-e^2\right)^{1/2}}X-\lambda_\alpha\frac{1}{\left(1-e^2\right)^{1/2}}\frac{R^3}{\mu}\left[1-l_0\left(X^2+Y^2\right)^{-1/2}\right]X$$

$$Y''+2X'=-\frac{3k_2}{R^2}\frac{1}{\left(1-e^2\right)^{1/2}}Y-\lambda_\alpha\frac{R^3}{\mu}\frac{1}{\left(1-e^2\right)^{1/2}}\left[1-l_0\left(X^2+Y^2\right)^{-1/2}\right]Y \tag{6}$$

To determine the equilibrium positions of the system, we will restrict the system's position by fixing constant co-ordinates. Let the constant co-ordinates be denoted as

$$X = X_0, Y = Y_0 \tag{7}$$

Putting these values in equations (6) and doing some simple calculations, the equilibrium positions are obtained as

$$(X_0, Y_0) = \frac{(1-e^2)^{1/2}\left[A\cos i - \frac{\lambda_\alpha R^3}{\mu(1-e^2)^{1/2}} l_0 - \frac{R^3}{\mu}\left(\frac{B_1}{m_1} - \frac{B_2}{m_2}\right)\frac{\sin\theta}{\pi}\right]}{(3 + \frac{12k_2}{R^2} - \lambda_\alpha \frac{R^3}{\mu})}, 0 \tag{8}$$

5. Stability of the Equilibrium Positions

To test the stability of the equilibrium positions of the tether satellite system under the mentioned perturbative forces, the equations (5) are rewritten in the case of maximum effect of earth's shadow and thus putting $\epsilon = 0$ and $\alpha = 0$ to these equations, the equations becomes

$$X'' - 2Y' - \frac{3X}{(1-e^2)^{1/2}} = -A\cos i + \frac{R^3}{\mu}\left(\frac{B_1}{m_1} - \frac{B_2}{m_2}\right)\frac{\sin\theta}{\pi} + \frac{12k_2}{R^2}\frac{1}{(1-e^2)^{1/2}}X - \lambda_\alpha \frac{1}{(1-e^2)^{1/2}}\frac{R^3}{\mu}\left[1 - l_0\left(X^2 + Y^2\right)^{-1/2}\right]X$$

$$Y'' + 2X' = -\frac{3k_2}{R^2}\frac{1}{(1-e^2)^{1/2}}Y - \lambda_\alpha \frac{R^3}{\mu}\frac{1}{(1-e^2)^{1/2}}\left[1 - l_0\left(X^2 + Y^2\right)^{-1/2}\right]Y \tag{9}$$

Now, small variations about the co-ordinates of the equilibrium positions are taken and applied to equations (9). Let the variations be represented by

$$X = X_0 + \Delta_1$$
$$Y = Y_0 + \Delta_2 \tag{10}$$

Applying these variations to equations (9), the set of equations becomes

$$\Delta_1'' - 2\Delta_2' - \frac{3(X_0 + \Delta_1)}{(1-e^2)^{1/2}} = -A\cos i + \frac{R^3}{\mu}\left(\frac{B_1}{m_1} - \frac{B_2}{m_2}\right)\frac{\sin\theta}{\pi} + \frac{12k_2}{R^2}\frac{(X_0 + \Delta_1)}{(1-e^2)^{1/2}} - \frac{\lambda_\alpha R^3}{\mu(1-e^2)^{1/2}}\left[1 - l_0[(X_0 + \Delta_1)^2 + \Delta_2^2]^{-1/2}\right](X_0 + \Delta_1)$$

$$\Delta_2'' + 2\Delta_1' = -\frac{3k_2}{R^2}\frac{\Delta_2}{(1-e^2)^{1/2}} - \frac{\lambda_\alpha R^3}{\mu(1-e^2)^{1/2}}\left[1 - l_0[(X_0 + \Delta_1)^2 + \Delta_2^2]^{-1/2}\right]\Delta_2 \tag{11}$$

Equations (9) admit a Jacobean integral, so their variational equations (11) also constitute a Jacobean integral. The form of the Jacobean integral in the variational parameters is given by

$$\Delta_1'^2 + \Delta_2'^2 - \left[\frac{2\lambda_\alpha R^3}{\mu(1-e^2)^{1/2}} l_0 - \frac{2\lambda_\alpha R^3}{\mu(1-e^2)^{1/2}} X_0 + \frac{6X_0}{(1-e^2)^{1/2}} - 2A\cos i + \frac{2R^3}{\mu}\left(\frac{B_1}{m_1} - \frac{B_2}{m_2}\right)\frac{\sin\theta}{\pi} + \frac{24k_2}{R^2}\frac{X_0}{(1-e^2)^{1/2}}\right]\Delta_1 +$$
$$\left[\frac{3k_2}{R^2(1-e^2)^{1/2}} + \frac{\lambda_\alpha R^3}{\mu(1-e^2)^{1/2}}\right]\Delta_2^2 + \left[\frac{3}{(1-e^2)^{1/2}} - \frac{12K_2}{R^2(1-e^2)^{1/2}} + \frac{\lambda_\alpha R^3}{\mu(1-e^2)^{1/2}}\right]\Delta_1^2 = h \tag{12}$$

where, *h* is the Jacobean constant. To test the stability, Lyapunov's method is now applied to the Jacobean integral equation. This integral equation is considered as Lyapunov's function $L(\Delta_1', \Delta_2', \Delta_1, \Delta_2)$. Thus

$$L(\Delta_1',\Delta_2',\Delta_1,\Delta_2)=\Delta_1'^2+\Delta_2'^2-\left[\frac{2\lambda_\alpha R^3}{\mu\left(1-e^2\right)^{1/2}}l_0-\frac{2\lambda_\alpha R^3}{\mu\left(1-e^2\right)^{1/2}}X_0+\frac{6X_0}{\left(1-e^2\right)^{1/2}}-2A\cos i+\frac{2R^3}{\mu}\left(\frac{B_1}{m_1}-\frac{B_2}{m_2}\right)\frac{\sin\theta}{\pi}+\frac{24k_2}{R^2}\frac{X_0}{\left(1-e^2\right)^{1/2}}\right]\Delta_1$$
$$+\left[\frac{3k_2}{R^2\left(1-e^2\right)^{1/2}}+\frac{\lambda_\alpha R^3}{\mu\left(1-e^2\right)^{1/2}}\right]\Delta_2^2+\left[\frac{3}{\left(1-e^2\right)^{1/2}}-\frac{12K_2}{R^2\left(1-e^2\right)^{1/2}}+\frac{\lambda_\alpha R^3}{\mu\left(1-e^2\right)^{1/2}}\right]\Delta_1^2 \tag{13}$$

The Lyapunov function $L(\Delta_1',\Delta_2',\Delta_1,\Delta_2)$ is the integral of the variational equations (11), and its differentiation taken along the trajectory of the system must vanish identically. The only condition for this is that the Lyapunov function must be positive definite. To make equation (13) positive definite, the first order variable terms should be zero. In fact, these conditions imply the position of the equilibrium position. The second order terms must satisfy Sylvester's conditions for positive definiteness. So, the sufficient condition becomes,

(i) $$\frac{2\lambda_\alpha R^3}{\mu\left(1-e^2\right)^{1/2}}l_0-\frac{2\lambda_\alpha R^3}{\mu\left(1-e^2\right)^{1/2}}X_0+\frac{6X_0}{\left(1-e^2\right)^{1/2}}-2A\cos i+\frac{2R^3}{\mu}\left(\frac{B_1}{m_1}-\frac{B_2}{m_2}\right)\frac{\sin\theta}{\pi}+\frac{24k_2}{R^2}\frac{X_0}{\left(1-e^2\right)^{1/2}}=0$$

(ii) $$\frac{3}{\left(1-e^2\right)^{1/2}}-\frac{12K_2}{R^2\left(1-e^2\right)^{1/2}}+\frac{\lambda_\alpha R^3}{\mu\left(1-e^2\right)^{1/2}}>0$$

(iii) $$\frac{3k_2}{R^2\left(1-e^2\right)^{1/2}}+\frac{\lambda_\alpha R^3}{\mu\left(1-e^2\right)^{1/2}}>0$$

The equilibrium condition shows that the Y centroid orbit coordinate is zero. This indicates the tether coincides with the orbital plane, with the centre of mass and mass point of m_1 and m_2 are collinear with the centre of mass of the earth. However, this equilibrium position is not stable because the sufficient conditions for the stability are not satisfied simultaneously. To stabilize the orbit, a different control method is required, which is part of the further tether satellite research. In literature [25], the authors studied the stability of tethered satellites system and calculated the equilibrium positions in which they concluded that the tether is perpendicular to the orbital plane or coincided with the orbital plane in the central gravitational field of earth ignoring the elasticity of the cable. The authors also calculated the necessary and sufficient condition of the maximum extent for the system equilibrium can reach, which occurs in a circular orbit. In references [26,27], the authors determined the equilibrium positions of the system, taking the effect of air drag. Under such conditions, the Y co-ordinate of the system has definite value. The non-availability of the generalized perturbative forces experimental data restricts us the stability analysis using graphical method. For a short period of time, other perturbative forces may be neglected, and the problem can be considered only under the effect of central gravitational field of earth. Then the graphs drawn with true anomaly (ν) vs. rotating co-ordinate (ξ) taking the tether length unity are shown in Figs. 2 and 3.

With reference to ξ equal to one, the graph is divided into two regions. In some phases, the system is in a region where ξ is greater than one, and in other phases, the system is in a region where ξ is less than one. The value ξ greater than one represents an unstable equilibrium positions, as the condition of constraint is not satisfied at the equilibrium positions. The region where ξ is less than one represents the stability region of the system, where the condition of constraint is satisfied, and the dynamics to control the system is easier compared to the previous case.

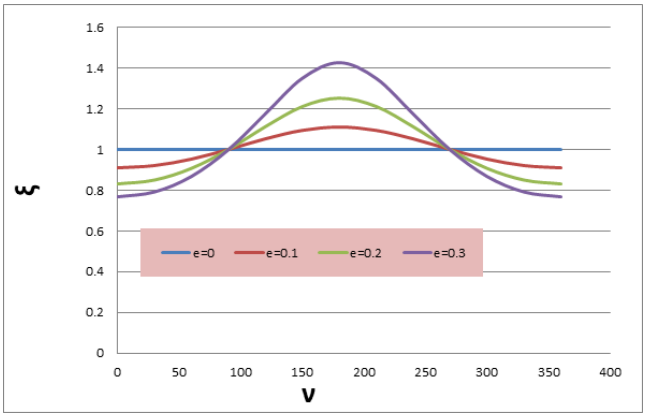

Fig. 2. Plots of ν vs. ξ for different eccentricities.

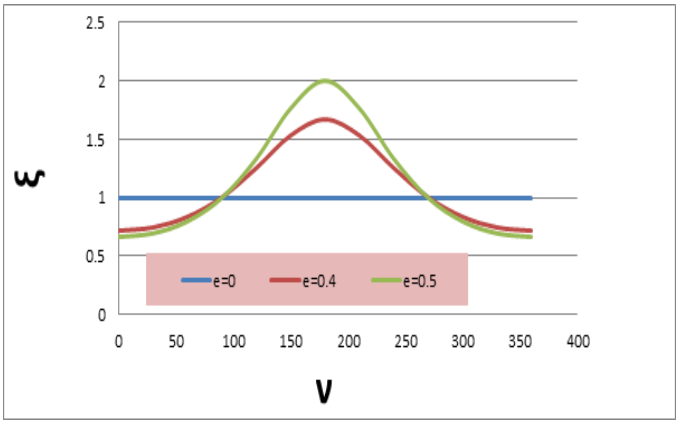

Fig. 3. Plots of ν vs. ξ for different eccentricities.

4. Conclusion

In this study, the dynamical behavior of tethered satellites has been analyzed under the influences of several perturbative forces. By differentiating the X-coordinate of the equilibrium positions with respect to the eccentricity of the orbit, it is easy to show that the

extension of the equilibrium position is maximum for a zero eccentric orbit (circular) compared to any other orbits. The equilibrium condition also shows that the Y centroid orbit coordinate is zero. This indicates that the tether coincides with the plane of the orbit, with the centre of mass and mass point m_1, m_2 are collinear with the centre of mass of earth. It is concluded that the equilibrium positions of the non-linear motion of a tether connected satellites system is unstable in the sense of Lyapunov, taking into account the elasticity and the influence of other general perturbative forces, such as earth's magnetic field, solar radiation pressure, shadow of the earth and earth's oblateness. By neglecting other perturbative forces in the graphical analysis, it is concluded that during certain phases of motion, the system resides in a stable region, where controlling the system is easier compared to the unstable regions. The system's motion, including its elastic vibration, is generally unstable in circular orbits. Instability is caused by an energy inflow into the pendulous motion from the earth's magnetic field at the expense of action of a non-conservative force.

References

1. K. E. Tsiolkovsky, Speculations Between Earth and Sky (Isd-voAN-SSSR, Moscow, 1895) pp. 35.
2. D. D. Lang and R. R. Nolting, Gemini Summary Conference (Houston, Texas, NASA SP, 1967) **138**, pp. 55-66.
3. V. V. Beletskii , M. B. Ivanov, and E. I. Otstavnov, Cosmic Res. **43**, 152 (2005). https://doi.org/10.1007/s10604-005-0029-1
4. B. C. Edwards, The Space Elevator NIAC Phase II Final Report (March 1, 2003). http://images.spaceref.com/docs/spaceelevator/521Edwards.pdf
5. V. V. Beletsky and E. N. Levin, Adv. Astron. Sci. **83**, 267 (1993).
6. E. L. M. Lanoix, A Mathematical Model of the Long Term Dynamics of Tethered Spacecraft, Monreal (McGill University, Montreal, Quebec, 1999).
7. M. Kurpa, W. Poth, M. Sxhagerl, A. Stendl, W. Steiner, H. Treger, and G. Wiedermann, Non-linear Dynamics **43**, 73 (2006). https://doi.org/10.1007/s11071-006-0752-z
8. A. Khan and N. Goel, Int. J. Contemp. Maths. Sci. **6**, 299 (2011).
9. S. Kumar and J. D. Prasad, Indian J. Theo. Phys. **63**, 1 (2015).
10. S. Kumar and S. Kumar, Int. J. Astro. Astrophys. **6**, 288 (2016). https://dx.doi.org./10.4236/ijaa.2016.63024
11. S. Kumar, J. Phys. Sci. **23**, 165 (2018). https://doi.org/10.1002/ajpa.23384
12. A. A. Burov and H. Troger, J. Appl. Math. Mech. **64**, 723 (2000). https://doi.org/10.1016/S0021-8928(00)00101-5
13. M. R. Liberzon, Automation Remote Control **67**, 1610 (2006). https://doi.org/10.1134/S0021-8928(00)00101-5
14. B. S. Yu, H. Wen, and D. P. Jin, Acta Mechanica Sinica **34**, 754 (2017). https://doi.org/10.1007/s10409-018-0752-5
15. B. S. Yu, S. D. Xu, and D. P. Jin, Nonlinear Dynamics **101**, 1233 (2020). https://doi.org/10.1007/s11071-020-05844-8
16. D. J. McKenzie, Ph.D. Thesis, University of Glasgow, UK, 2010.
17. A. A. Malashin, N. N. Smirnov, O. Y. Bryukvina, and P. A. Dyakov, J. Sound Vib. **389**, 41 (2017). https://doi.org/10.1016/j.jsv.2016.11.026
18. W. Jung, A. P. Mazzoleni, and J. Chung, Nonlinear Dynamics **82**, 1127 (2015). https://doi.org/10.1007/s11071-015-2221-z

19. J. Pelaez and Y. N. Andres, J. Guid., Control, Dynamics **28**, 611 (2005). https://doi.org/10.2514/1.6685
20. P. Williams, C. Blanksby, and P. Trivailo, Acta Astronautica **53**, 681 (2003). https://doi.org/10.1016/S0094-5765(03)80029-2
21. K. K. Mankala and S. K. Agrawal, J. Vib. Acoust. **130**, ID 014501 (2008). https://doi.org/10.1115/1.2776342
22. K. K. Mankala and S. K. Agrawal, J. Vib. Acoust. **127**, 144 (2005). https://doi.org/10.1115/1.1891811
23. B. S. Yu, H. Wen, and D. P. Jin, Chin. J. Theor. Appl. Mech. **42**, 926 (2010).
24. S. Kumar and J. Ghosh, Sci. Technol. J. **9**, 14 (2021). https://doi.org/10.22232/stj.2021.09.01.03
25. H. Yong, B. Liang, and W. Xu, Acta Astron. **68**, 1964 (2011). https://doi.org/10.1016/j.actaastro.2010.11.015
26. S. Kumar, J. Phys. Sci. **23**, 165 (2018). https://doi.org/10.1111/resp.13420_209
27. S. Kumar and A. Kumar, J. Sci. Res. **65**, 290 (2021). https://doi.org/10.37398/JSR.2021.650138